Estimation of *Lg*-coda Q value for the Northern Indian Ocean region based on spectral analysis

Prasanna Gamage[1], Dr. Srikanth Venkatesan[2]

1. Corresponding Author. PhD student, School of Engineering and Science, Victoria University, Australia.
   Email: janakaprasanna.wepitiyagamage@live.vu.edu.au

2. Senior Lecturer, School of Engineering and Science, Victoria University, Australia. Email: srikanth.venkatesan@vu.edu.au

Abstract

Attenuation of ground motion amplitudes with distance is recognised as a significant issue by researchers. Of particular interest is the attenuation or propagation of seismic waves from long distant sources. Regions like Sri Lanka have experienced tremors from events as far as 1500 km. However a comprehensive study of the region with respect to the propagation or attenuation of seismic waves has been generally lacking. With the availability of new archival data of 65 events recorded at Pallekelle Broadband station, the authors have estimated *Lg*-coda Q values for the Northern Indian Oceanic region surrounding Sri Lanka. Multiple linear regression analysis of recorded data yields a relatively higher Q value which is comparable to similar older crustal regions such as Western Australia and Central Europe. Source spectra for recorded events have also been accounted by correcting the observed amplitude for geometric and anelastic attenuation. This results in typical stress drop values of about 100 bars which is consistent with Brune's source spectra. Based on the estimated values, stochastic modelling of a recent 8.6 M_w event experienced in the region has been undertaken. Initial results are promising. Further analysis would establish reliable attenuation behaviour around the region.

Keywords: *Lg*-coda Q value, Regression analysis, Source spectra, Stochastic method, attenuation, ground motion.

1.0 INTRODUCTION

Earthquakes present a serious threat of natural hazard to mankind all over the world. However regions like Sri Lanka and Australia are generally ascertained as being away from plate boundaries with low levels of seismic risk. Sri Lanka is located in the Northern Indian Ocean more than a thousand kilometres away from major plate boundaries such as Sunda Arc subduction zone and Sumatran fault to the east and transformed faults of the Northern extension of Central Indian Ridge to the west. Therefore, the risk of direct inter-plate activities may be assumed to be low whilst secondary hazards like a tsunami cannot be avoided as seen in the case of a mega tsunami which resulted in the aftermath of the Aceh earthquake in 2004. Although the tsunami resulted in considerable awareness, very few local studies have since been undertaken so far in relation to seismic hazard studies. Furthermore, after the tsunami Sri Lanka did experience ground shaking from long-distant earthquakes from the far-away plate boundaries. Recognising the growing need to understand seismic risks, this paper is an attempt to study the attenuation behaviour of the region since it is an important part of assessing seismic hazard.

Historical seismicity of the Sri Lankan region can be studied as local and regional seismicity, considering events that occurred within the country and outside the country. Whilst, those that occurred within the country were poorly recorded, events that occurred outside the country were properly recorded in international archival databases such as ISC (International Seismological Centre-UK), ANSS (Advanced National Seismic System-USA). Hence, the latter provides essential information in identifying the possible intra-plate seismic nature around Sri Lanka. As evidenced by the above databases, shallow focus intra-plate earthquakes generated due to internal deformations of the Northern Indian Oceanic crust are in abundance especially in the Oceanic crust towards South-Eastern direction close to Ninety and Eighty-five east ridges (Figure 1a). A considerable number of studies have been carried out in the international context by a number of researchers (Stein and Okal, 1978; Weins et al, 1986; Royer and Gordon, 1997, etc.) in understanding the seismo-tectonic nature around these regions. The studies led to the identification of a large diffusing area within the Indo-Australian plate having a thinner lithospheric crust, which undergoes extensive internal compression due to thrust by surrounding regions, (Figure 1b). Hence, the equatorial region enclosed between the Central Indian ridge to the west and the Sumatra trench to the east, provides a prominent example of an active intra-plate area. The occurrence of several strong earthquakes with magnitude greater than 6-7 M_w during past decades including the recent M_w 8.6 and M_w 8.2 in April 2012, makes the region distinctive in respect to other oceanic crusts which have lower seismicity except at the continental margins or plate boundaries. According to some literature (Royer and Gordon, 1997) the minimum site-source distance between Sri Lanka and this identified diffusing area is less than 400km, which cannot be considered as a safe distance in terms of the level of seismicity of the region. Recent events (April 2012) noted above caused perceivable shakings in several places in Sri Lanka including the capital Colombo which is about 1500 km away from the epicentres. Accelerograms recorded at Pallekelle rock broadband station produced horizontal Peak Ground Acceleration (PGA) of the order of about 15 and 3 mm/s^{-2} for M_w 8.6 and M_w 8.2 events, respectively. These values can be accentuated several times by underlying sub-soil conditions. Hence, the risk of a large magnitude intra-plate earthquake generated in the oceanic crust surrounding the country cannot be ignored.

In the present study, authors have undertaken research to estimate the *Lg*-coda *Q* value representing the Northern Indian Oceanic crust surrounding Sri Lanka by analysing digital broadband vertical component records of 65 intra-plate earthquakes occurred surrounding the country (Figure 1a and Appendix). The finding has been further verified by matching real records with stochastically simulated seismograms employing estimated seismological parameters for the subject region.

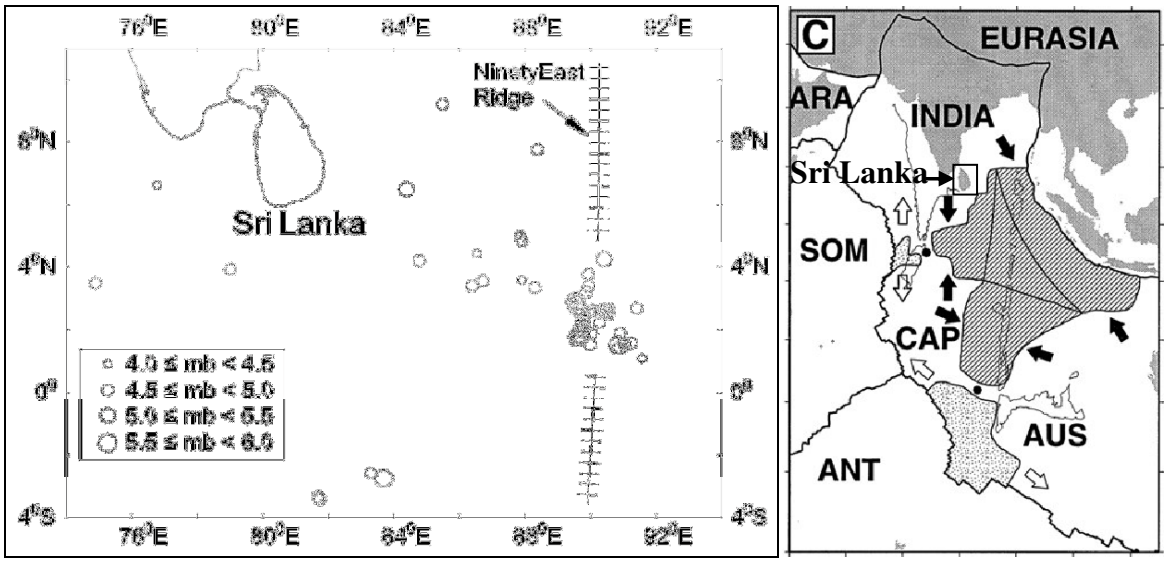

(a) (b)

Figure 1: Seismicity surrounding Sri Lanka: (a) Selected events for the analysis (Source; ANSS); (b) Large diffusing area (Hatched) located amidst trisected Indo-Australian plate (After Royer and Gordon, 1997)

2.0 DATA BASE AND THE PROCESSING PROCEDURE

Geological Survey and Mines Bureau (GSMB) of Sri Lanka, has been in collaboration with United States Geological Survey (USGS) for maintaining a broadband seismic station located at Pallekele since the year 2000. Digital waveforms of recorded events at the station are available to download from the respective data management system, i.e., IRIS data management centre. 65 such records of shallow crustal earthquakes with magnitude ranging from m_b 4.0 to m_b 5.7 have been downloaded and processed for further analysis. Location and magnitude data were directly obtained from ANSS global catalogue in which events are mostly available in body wave magnitude scale. Hence, the same magnitude type was chosen for the regression formula. One of events which was not available in m_b in ANSS data archive, was searched in ISC catalogue and was assigned the magnitude in m_b from global centroid moment tensor data to maintain the consistency of the data set. Epicentral distance varies from 2.7^0 (304 km) to 13.2^0 (1469 km) for the whole data set. The data base consists of a large number of records from aftershocks of the recent 8.6 M_w earthquake, which occurred on the 11th April 2012 in Indian Ocean, and this in turn strengthened the data set by increasing the original sample size. Magnitude and location uncertainties were omitted in all newer records though in some cases only quick preliminary determinations were available in ANSS data archive. On the other hand, the authors believe such an uncertainty would not be able to produce any notable deviations in the final important steps since most of the newer events were from a long distance of the order of about 500 km at least.

Broadband high gain vertical component data (BHZ) were selected in each of the wave form records. Since, there are two seismometers installed at two different depths

(one at 1 m and the other at 90 m depth) in the same rock, vertical components corresponding to both were selected in order to verify the results against any upper crustal modification effects. Horizontal components were not considered in the process as to avoid or to reduce local site amplification effects, which can be significant sometimes at high frequencies producing extensive variations in the horizontal motion. Vertical motion is said to be less affected by near-source upper crustal modifications (in terms of attenuation and amplification) by which offsetting any decay in wave propagation velocity with refracted waves travelling in the vertical direction (Atkinson, 2004). Selected vertical components were bandpass filtered between 0.1 – 9.0 Hz frequencies after applying tapering of 10% at both ends of the trace. The maximum frequency 9.0 Hz was selected in such a way that the maximum frequency limit should be less than half of the sample rate of the instrument; in the current case they were 20 and 40 sps for seismometers at 90 and 1 m depth, respectively (Ottemoller and Havskov, 2012). Next, filtered traces were corrected for instrument to produce acceleration time histories, followed by Fourier Acceleration Spectra (FAS) of each processed record by selecting the "shear/strong window" containing multiply reflected and refracted *S* and *Lg* phases. FAS were visually inspected for signal strength relative to the background noise spectra and amplitudes of frequencies 0.1, 0.2 and 0.3 Hz were left out owing to low frequency noise amplifications. FAS were smoothed for the selected whole frequency range at 0.1 log frequency bins by introducing a box/rectangular weighting function and thus taking geometric average of amplitudes in each frequency bin. This frequency dependent smoothing (due to constant width in log frequency) allows uniform smoothing of amplitudes over the entire frequency range in the log frequency scale. Although box weighting smoothing has shown little chatter at low frequencies with respect to other smoothing options (such as triangular weighting), the effect can be negligible in practical situations (Boore, 2012). Acceleration amplitudes of smoothed spectra in each vertical record were then tabulated in 0.1 Hz frequency increments for the selected frequency range. All the processing steps except smoothing have been done by using SEISAN (Havskov and Ottemoller, 2012), whereas the smoothing has been accomplished by using TSPP (Boore, 2012) data processing tools.

We fit the following well-established attenuation model (Atkinson and Mereu, 1992) with observed Fourier amplitudes by using the multiple linear regression.

$$[A_x(f)]_{ij} = [S(f)]_i . G . A_n(f) \tag{1}$$

Where, $[A_x(f)]_{ij}$ is the acceleration amplitude of Fourier spectra at jth station (in this case it is always "1") due to ith event for a given frequency f. $[S(f)]_i$ is the acceleration amplitude of Fourier spectra of ith event at the source. G and $A_n(f)$ are geometric attenuation factor and anelastic whole path attenuation factor, respectively, having the following relations;

$$G = \frac{R_0}{1.5D}\sqrt{\frac{2.5D}{R}} \qquad \text{for } R > 2.5D \tag{2}$$

$$A_n(f) = e^{\frac{-\pi f R}{Q\beta}} \tag{3}$$

Here, D, R, f, Q and β are crustal thickness, epicentral distance, wave frequency, wave transmission quality factor, and shear wave velocity at the source region,

respectively. R_0 is equal to 1 km. Geometric attenuation noted in equation (2) for long distant earthquakes are generally apportioned as R^{-1} up to 1.5D distance due to spherical spreading near the source area, zero attenuation between 1.5D and 2.5D due to compensatory effect of postcritical reflections and refractions from Moho and Conrad discontinuities and $R^{-0.5}$ rate for cylindrical attenuation after 2.5D due to multiple reflections and refractions of body waves dominating *Lg* phase in the shear window of the trace (Lam et al, 2000, Atkinson and Boore, 1995). Atkinson, 2004 and Sonley, 2004 have also reported a more rapid attenuation of $R^{-1.3}$ as opposed to R^{-1} in the near source region and a negative attenuation of $R^{+0.2}$ instead of zero attenuation in the 1.5D and 2.5D distance. Since these are derived for regions such as south-eastern Canada the authors have adopted geometric attenuation factors as denoted in equation (2) to be consistent with atypical stable regions such as Australia, south China and Singapore. Crustal thicknesses, D values, near the source areas in the oceanic crust surrounding the country were determined using the global crustal model called CRUST2.0 (2001) in which average crustal thicknesses all over the world are compiled to represent in 2^0 x 2^0 tiles. The value of 10 km was inferred for most of the parts in Northern Indian Oceanic crust by referring to the data from CRUST2.0 as well as by considering hypocentral depth values given in catalogues for selected events. Equation (3) denotes attenuation of waves as a result of energy dissipation along the whole travel path during wave propagation through the rock medium. This energy dissipation entails heating of the heterogeneous medium and rearrangement/dislocation of particles during vibration of the medium, which are considered as permanent losses of energy. Moreover, whole path attenuation or seismic absorption depends on wave frequency in a manner in which high frequency waves are diminishing more rapidly than low frequency waves and the decay has an exponential form, as can be seen in Eq. (3). The reason can be explained by analogizing the situation with frequency dependent amplitude decay of wave motion in an elastic medium due to viscous damping, in which the decay rate increases with number of wave cycles in a unit length (frequency). Importantly, the whole path attenuation is dominant in distant earthquakes in which the amount of attenuation is largely dependent on the crustal quality of the travelled medium. If the rock quality is high, the wave propagation is good and vice versa. Hence, the wave transmission quality of the rock, parameterized as Q (or, Q_0 equals to Q at 1 Hz frequency), is a key parameter to be estimated correctly for long-distant events i.e. for regions like Sri Lanka.

$[S(f)]_i$, which denotes FAS at the source for a given frequency, depends significantly on the magnitude of the event and the typical stress drop level ($\Delta\sigma$) of the subject region which can be considered to remain constant for any magnitude except smaller magnitudes ($M < 4.3$) in which $\Delta\sigma$ has shown an increasing trend with the magnitude (Atkinson, 2004). Furthermore, Stable Continental Regions (SCRs) have shown comparably higher stress drop values than that of active regions located close to plate boundaries (Lam et al, 2000). During the regression analysis the magnitude dependency (which comes through the source term) of observed FAS at the recording station has been nullified by employing an assumed second order polynomial relationship between the source term and the magnitude as follows;

$$\log[S(f)]_i = C_1(M-4)^2 + C_2(M-4) + C_3 \quad (4)$$

Where M is the magnitude in m_b and C_1 to C_3 are constants to be determined from the regression. Equation (4) decouples magnitude dependency of the regression equation and hence enables us to perform the analysis for the whole data set simultaneously

over the entire magnitude range without considering each magnitude independently (Joyner and Boore, 1981; Atkinson, 2004). Moreover, this decoupling technique is advantageous since it minimizes errors in regression coefficients which can arise due to magnitude uncertainties associated especially with newer events, and it also curtails the total number of analysis steps of the regression process by eliminating repetitive ones. Substituting terms of equations (2), (3) and (4) in (1) and taking logarithms give the following attenuation equation for regressions;

$$\log[A_x(f)]_{ij} = C_1(M-4)^2 + C_2(M-4) + C_3 - \log[1.5D] - 0.5\log[\frac{R}{2.5D}] - [\frac{\pi f \log e}{Q\beta}]R \quad (5)$$

In the above attenuation model, wave modifications at the upper crustal level in terms of attenuations and amplifications have been neglected. The reason for this is based on the consideration of the underlying rock stratigraphy in the Sri Lankan region. A number of sources indicate more than 90% of Sri Lanka's upper crustal rock layer consists of Crystalline rocks of Precambrian age in which the age can be as old as about 2000 Ma (Kroner and Brown, 2005; Cooray, 1994). Therefore, wave propagation in the upper 3-4 km would be less affected by poor rock quality characteristics as would be the case for younger Sedimentary rocks. This can further be explored by comparing recorded amplitudes at two different depths (discussed later) at the station. The average shear wave velocity of source regions within the oceanic crust was taken as 3.9 km/s based on CRUST2.0 data. Results of the multiple linear regressions and estimated *Lg*-coda Q values are discussed in next section.

3.0 RESULTS AND DISCUSSION

Regression coefficients C_1 through to C_3 and Q values for each 0.1 Hz frequency increment in the whole frequency range of 0.1 to 9.0 Hz have been determined by the regression. Estimated values for certain selected frequencies, pertaining to both depth categories (90 and 1 m) along with their respective correlation coefficients (R^2) and Standard Error of Estimates (SEEs) are tabulated in Table 1.

	For vertical components at 90m depth						***For vertical components at 1m depth***					
f	C_1	C_2	C_3	C_4	R^2	SEE	C_1	C_2	C_3	C_4	R^2	SEE
0.4	0.631	-0.340	-0.650	-0.00068	0.62	0.26	0.623	-0.312	-0.861	-0.00065	0.58	0.29
0.5	0.663	-0.268	-0.808	-0.00061	0.72	0.24	0.641	-0.213	-0.998	-0.00061	0.66	0.28
0.6	0.541	0.029	-0.791	-0.00071	0.73	0.25	0.515	0.094	-0.988	-0.00070	0.68	0.29
0.7	0.461	0.189	-0.842	-0.00070	0.70	0.27	0.434	0.251	-1.042	-0.00068	0.65	0.30
0.8	0.436	0.289	-0.893	-0.00063	0.70	0.28	0.407	0.353	-1.091	-0.00061	0.66	0.31
0.9	0.437	0.299	-0.751	-0.00071	0.72	0.27	0.407	0.366	-0.943	-0.00070	0.69	0.30
1	0.413	0.320	-0.684	-0.00077	0.71	0.27	0.379	0.394	-0.875	-0.00076	0.69	0.29
2	0.407	0.162	0.009	-0.00110	0.71	0.26	0.367	0.245	-0.165	-0.00111	0.67	0.29
3	0.359	0.196	0.286	-0.00141	0.75	0.25	0.310	0.301	0.157	-0.00144	0.71	0.28
4	0.410	0.081	0.563	-0.00169	0.74	0.28	0.325	0.259	0.512	-0.00177	0.69	0.33
5	0.463	-0.077	0.642	-0.00176	0.74	0.28	0.299	0.258	0.727	-0.00192	0.66	0.36
6	0.616	-0.345	0.487	-0.00164	0.75	0.27	0.274	0.346	0.861	-0.00205	0.64	0.41
7	0.740	-0.618	0.275	-0.00147	0.74	0.25	0.168	0.540	1.010	-0.00222	0.63	0.44
8	1.070	-1.261	-0.113	-0.00111	0.61	0.31	0.229	0.425	1.112	-0.00228	0.62	0.46
9	1.199	-1.522	-0.716	-0.00088	0.55	0.33	0.275	0.323	1.155	-0.00232	0.62	0.46

Table 1: Regression coefficients (C_1, C_2, C_3 and C_4=$\pi f \log e/(Q\beta)$) of the equation (5) for observed FAS at 90 and 1 m depth along with their respective correlation coefficient (R^2) and Standard Error of Estimate (SEE) for selected frequencies.

The regression has resulted in a good match as shown in Figure 2 with even a better match for the 90 m depth case. This is also confirmed in Table 1, as indicated by the higher correlation coefficients and lower SEEs. Figure 2 presents a comparison of recorded Fourier amplitudes with predicted ones by the attenuation equation (5) for the magnitude range of 4.5-5.0 m_b.

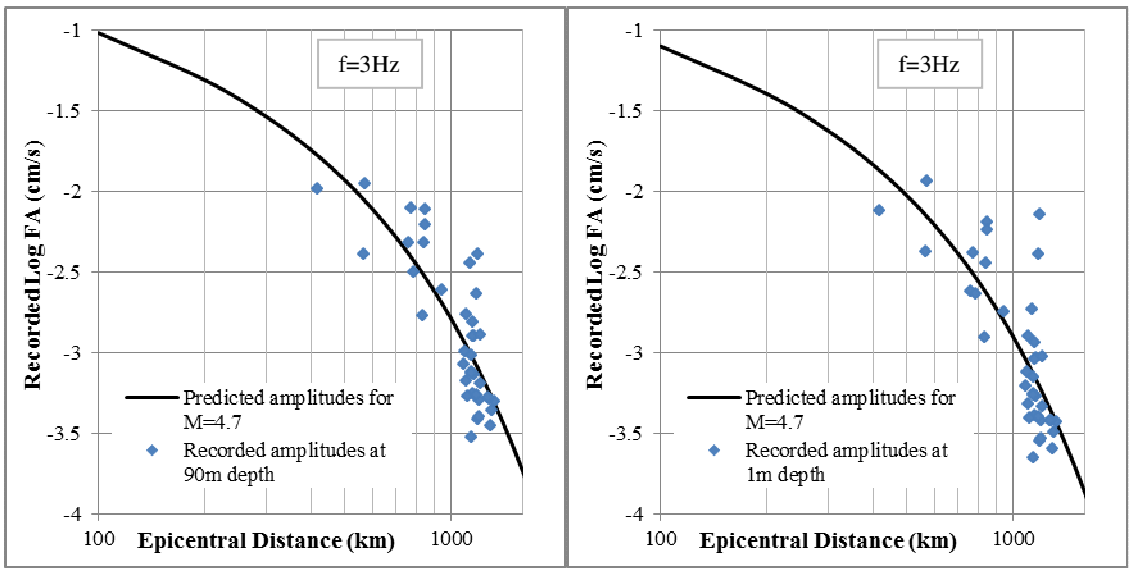

(a) (b)

Figure 2: Comparison of recorded amplitudes with predicted amplitudes by equation (5) for 3Hz frequency: (a) For records at 90 m depth; (b) For records at 1 m depth

Frequency dependent Q values were estimated from the regression coefficient relevant to the anelastic attenuation term, and then values were fit to the following logarithmic relationship using the method of the least squares. Here, Q_0 equals Q at 1 Hz frequency and n is called the "exponent". Both these parameters are related to the wave transmission quality of the underlying rock of the region in terms of intrinsic attenuation (as discussed above) and/or the amount of scattering due to wave reflection and refraction in the medium (Wu and Aki, 1988). Frequency dependent Q values with line of best fit to the equation (6) are shown in Figure 3.

$$\log Q = n \log f + \log Q_0 \qquad (6)$$

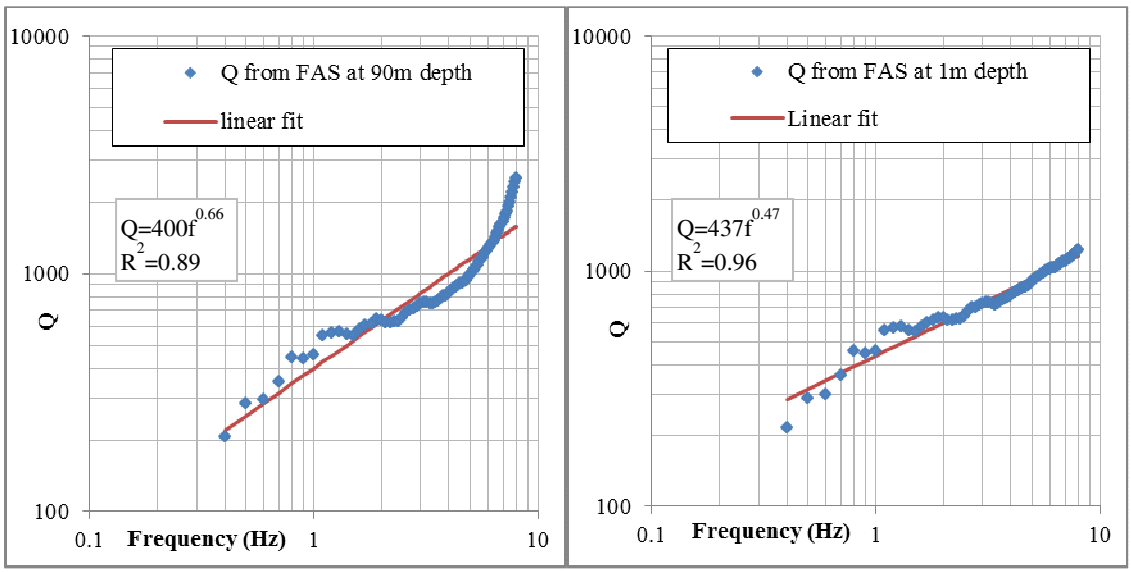

(a) (b)

Figure 3: Frequency dependent Q values estimated from the regression results: (a) For FAS at 90 m depth; (b) For FAS at 1 m depth

Q values fore frequencies greater than 8 Hz were not considered for the linear fit owing to comparably higher SEEs and lower R^2. Relatively higher Q_0 values were found for both cases as expected whereas in 90 m case, slightly lower Q_0 resulted due to sudden ascent of Q values after about 5 Hz frequency. This higher Q_0 value is comparable with other typical older crustal regions such as Western Australia and Central Europe and can be attributed with the region's inherent seismotectonic nature, which comprises an older crustal rock straitigraphy having better wave propagation features. The country's geotectonic location set amidst in the centre of the Indo-Australian plate may further enhance this fact, since crust is getting older as close as to its centre than to plate boundaries. However, the authors believe that the inferred Q_0 should be represented not in the local context but in a regional context which includes both the continental crust lying under the country and the oceanic crust surrounding the country. Singh et al (2004) have also estimated a much higher *Lg*-coda Q value of about 800 for the neighbouring Indian Sheild region based of FAS analysis, which again is consistent with older crust in the region. On the other hand, one would argue that the lesser geometric attenuation due to thinner oceanic crust of the order of about 10 km surrounding the country, may sometimes lead to a higher Q_0 value, but this is not always the case since the geometric attenution (G) is a frequency independent parameter which reduces amplitudes by a constant amount in each frequency whereas "n - exponent" (in equation (6)) depends on the slope of the line and hence is frequency dependent. Comparably lower n (0.66 and 0.47 for 90 and 1 m, respectively) means lower attenuation and thereby higher Q_0.

The sudden ascent above about 5 Hz frequency shown in figure 3(a) needs an explanation. This is related to high frequency amplitude degradation at 90 m depth after about 5 Hz. Average ratio of amplitudes at 1 m to 90 m for a selected magnitude range (4.5-5.0 mb) is shown in Figure 4. This sudden spike is unlikely to link with uppercrustal site amplifications as it only limited to higher frequencies greater than 5 Hz. It remains constant close to 1 for all other frequencies. The authers believe the effect may be attributed to either high frequency noise contamination at the 1 m sensor close to the ground surface or due to different sampling rate issues (20 and 40 sps for 90 and 1 m depths, respectively) of the two sensors. This will be investigated later.

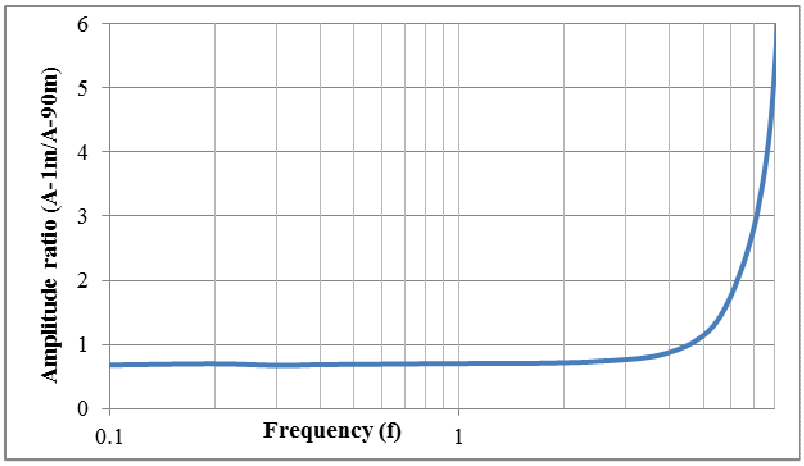

Figure 4: Average ratio of Fourier amplitudes between 1 m and 90 m for a selected magnitude range (4.5-5.0 mb)

The source spectra associated with recorded events can be examined by correcting the observed amplitude for geometric and anelastic attenuation so as to satisfy the following equation.

$$\log[A_s(f)] = \log[A_x(f)] + \log[1.5D] + 0.5\log[\frac{R}{2.5D}] + [\frac{\pi f \log e}{Q\beta}]R \qquad (7)$$

Here, the subscript "s" in the log amplitude term is to denote amplitude at "the source" and all other terms have their same meanings as aforementioned. This method of estimating source spectra may create bias sometimes especially in the current case since the amplitude correction has been done based on a single station. However, considering a range of similar magnitudes and thus estimating source spectra for a range of similar events, would give a primary estimate about source characteristics of the region. Estimated source spectra have been compared with Brune's source spectra (1970) with an average stress drop ($\Delta\sigma$) value of about 100 bar. 100 is reasonable for small to moderate magnitude events in a typical intra-plate region, though in some cases the value can be higher as indicated by Atkinson (2004) for Eastern North America (ENA). Brune's source model is given in equation (8);

$$[A_s(f)] = CM_0(2\pi f)^2 / [1 + (f / f_0)^2] \qquad (8)$$

Where, $C = 0.78/(4\pi\rho\beta^3)$ in which ρ and β are density (taken as 2800 kg/m^3) and shear wave velocity (taken as 3.9 km/s) of the source region, respectively. M_0 is the seismic moment. The corner frequency, $f_0 = 4.9\times10^6\,\beta(\Delta\sigma / M_0)^{1/3}$, when β, $\Delta\sigma$ and M_0 are in km/s, bars and dyne centimetres, respectively. The seismic moment of each event was estimated converting available body wave magnitudes (mb) by using following relationships (Kanamori, 1983; Abe, 1981);

$$\log M_0 = 2.4m_B + 10.1 \qquad \text{and} \qquad m_B = 1.5m_b - 2.2 \qquad (9)$$

Estimated average source spectra for recorded events having magnitude between 4.5-5.0 m_b along with Brune's model source spectra for typical 100 bar stress drop level are shown in Figure 5.

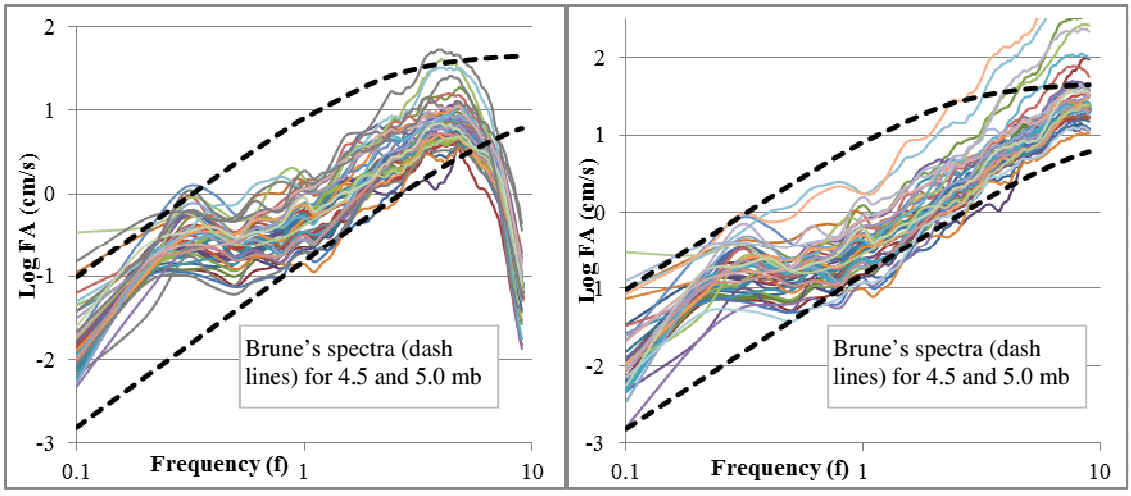

Figure 5: Average source spectra for recorded events (4.5-5.0 mb) with Brune's source spectra (dash lines): (a) For records at 90 m depth; (b) For records at 1 m depth

Source spectra lie within the limits of Brune's spectra for the selected range of magnitudes (i.e. 4.5-5.0 m_b) noting the average is closer to the lower bound. Moreover, high frequency source spectral amplitudes of records at 1 m depth better conform to Brune's source spectra than do records at 90 m depth. The reason may be associated with the sudden amplitude decay, which caused earlier sudden ascent in frequency dependent Q values, at high frequencies (above about 5 Hz) of records at 90 m depth. Despite this sudden amplitude decay problem, estimated source spectra show a good match with Brune's source spectra for typical 100 bar stress drop value. Hence, the frequency content and the general "shape" of the source spectrum in the subject region, has a conformity with the "generic source spectrum" developed for the ENA, which shows slightly higher stress drop levels than that of the present case. Subsequently, the final wave frequency content at the rock outcrop is little affected by changes in source spectrum characteristics for a particular magnitude of earthquake, since the final shape of the spectrum is governed mainly by modifications during the wave's travel through the rock medium in terms of attenuations and amplifications as described previously.

Finally, Ground motion on rock sites due to the recent 8.6 M_w event was artificially modelled using a theoretical based approach called "Stochastic Method" by employing the "seismological model" formulated in equation (1) with estimated Q_0 values using the regression as described above. Atkinson's typical double corner frequency ENA point source spectrum is used herein (Atkinson and Silva, 1997). Lam et al (2000) have combined the seismological model with the stochastic process to simulate seismograms to fit with the frequency contents defined by the model (a detailed description of the process is given in Lam et al (2000)). During the modelling we have omitted upper crustal modifications owing to higher wave propagation characteristics of the country's underlying near-surface basement rocks of Precambrian age. The shear wave velocity near rock outcrops for typical Sri Lankan Precambrian rocks is considered to be about 2.5 km/s (Jayawardena, 2001). The value shows consistency with shallow reference shear wave velocities of other Precambrian regions found in the world such as Western Australia, Canadian Shield, etc (Chandler, 2006). Hence, we believe the upper crustal modifications should be minimal in effect and can be safely neglected for the modelling purpose. Pseudo elastic spectral velocities of modelled ground motions along with recorded components at 90 m depth are shown in Figure 6 (1 m depth values are lesser than 90 m and hence not shown).

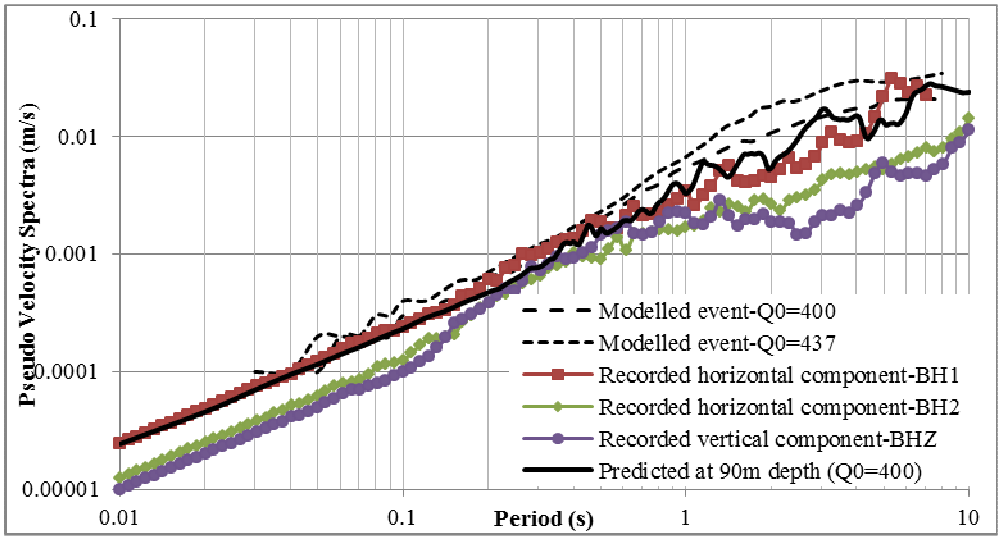

Figure 6: Recorded and modelled pseudo velocity spectra of 8.6M_w event at Pallekelle station.

Dotted and dashed lines show ensemble averages of the modelled ground motions, whereas the bold line shows the elastic spectra of the predicted ground motion at 90 m depth estimated using the one-dimensional equivalent linear method by performing back-analysis of the modelled ground motion (for Q_0 of 400) at the rock outcrop. Interesting consistency between modelled and recorded values can be seen from the figure 6, which in turn helps to verify the estimated Q_0 for the subject region in the Northern Indian Ocean.

4.0 CONCLUSION

Seismic wave transmission quality factor Q_0, for the Sri Lankan region including surrounding Northern Indian Ocean has been determined by using multiple linear regression analysis of FAS of 65 intra-plate earthquakes which occurred since 2000. Individual analysis of FAS recorded at two different depths (1 and 90 m) at the same station, resulted in higher Q_0 values which agree with the relatively older crustal rock stratigraphy of the subject region which has higher wave propagation features.

Upper crustal modifications (attenuation and amplification) during wave travel through the near-surface rock, have been omitted during both regression analysis and the stochastic modelling; this was considered unnecessary because of the country's underlying Precambrian Crystalline basement rock. Source spectra estimated by correcting the observed amplitude for geometric and anelastic attenuation show a good match with Brune's source spectra for a typical stress drop value of the order of about 100 bars. Stochastically modelled recent 8.6 M_w event for the estimated Q_0 values, shows a reasonable match with the actual records. It is acknowledged that the resulting correlation coefficients can be improved with further research, i.e. by considering a much larger database and by adopting more rigorous analysis techniques.

5.0 REFERENCES

- Abe, K. (1981). Magnitudes of large shallow earthquakes from 1904 to 1980. *Physics of the Earth and Planetary Interiors, 27*(1), 72-92.
- Advanced National Seismic System (ANSS), On-line catalogue. (2012). from http://www.ncedc.org/anss/catalog-search.html, United States Geological Survey
- Atkinson, G. M. (2004). Empirical Attenuation of Ground-Motion Spectral Amplitudes in Southeastern Canada and the Northeastern United States. *Bulletin of the Seismological Society of America, 94*(6), 2419-2423.
- Atkinson, G. M., & Boore, D. M. (1995). Ground-motion relations for eastern North America. *Bulletin of the Seismological Society of America, 85*(1), 17-30.
- Atkinson, G. M., & Mereu, R. F. (1992). The shape of ground motion attenuation curves in southeastern Canada. *Bulletin of the Seismological Society of America, 82*(5), 2014-2031.
- Atkinson, G. M., & Silva, W. (1997). An empirical study of earthquake source spectra for California earthquakes. *Bulletin of the Seismological Society of America, 87*(1), 97-113.
- Boore, D. M. (Cartographer). (2008, revised 2012). TSPP; a collection of FORTRAN programs for processing and manipulating time series: U.S. Geological Survey, Open-File Report 2008-1111.
- Brune, J. N. (1970). Tectonic stress and the spectra of seismic shear waves from earthquakes. *Journal of Geophysical Research, 75*(26), 4997-5009.

- Chandler, A. M., Lam, N. T. K., & Tsang, H. H. (2006). Near-surface attenuation modelling based on rock shear-wave velocity profile. *Soil Dynamics and Earthquake Engineering, 26*, 1004-1014.
- Cooray, P. G. (1994). The Precambrian of Sri Lanka: a historical review. *Precambrian Research, 66*, 3-20.
- Havskov, J., & Ottemo¨ller, L. (2012). SEISAN: The Earthquake Analysis Software for Windows, Solaris and Linux, Version 8.0.
- Institute of Geophysics and Planetary Physics. The University of California, S. D. (2001). Global Crustal Model CRUST2.0, http://mahi.ucsd.edu/Gabi/rem.dir/crust/crust2.html.
- International Seismological Centre (ISC), On-line Bulletin. (2012). from http://www.isc.ac.uk, Internatl. Seis. Cent., Thatcham, United Kingdom.
- Jayawardena, U. d. S. (2001). A Study of the Engineering Properties of Sri Lankan Rocks. *Engineer, Journal of Institution of Engineers, XXXIV*(2), 7-20.
- Joyner, W. B., & Boore, D. M. (1981). Peak horizontal acceleration and velocity from strong-motion records including records from the 1979 imperial valley, California, earthquake. *Bulletin of the Seismological Society of America, 71*(6), 2011-2038.
- Kanamori, H. (1983). Magnitude scale and quantification of earthquakes. *Tectonophysics, 93*(3-4), 185-199.
- Kroner, A., & Brown, L. (2005). Structure, Composition and Evolution of the South Indian and Sri Lankan Granulite Terrains from Deep Seismic Profiling and Other Geophysical and Geological Investigations: A LEGENDS Initiative. *Gondwana Research, 8*(3), 317-335.
- Lam, N., Wilson, J., & Hutchinson, G. (2000). Generation of synthetic earthquake accelerograms using seismological modelling: A review. *Journal of Earthquake Engineering, 4*(3), 321-354.
- Royer, J. Y., & Gordon, R. G. (1997). The motion and boundary between the Capricorn and Australian plates. *SCIENCE, 277*, 1268-1274.
- Singh, S. K., García, D., Pacheco, J. F., Valenzuela, R., Bansal, B. K., & Dattatrayam, R. S. (2004). Q of the Indian Shield. *Bulletin of the Seismological Society of America, 94*(4), 1564-1570.
- Sonley, E. (2004). *Investigation of earthquake attenuation in the Charlevoix, Quebec, seismic zone.* Ph.D. Thesis, Carleton University, Ottawa, Canada.
- Stein, S., & Okal, E. A. (1978). Seismicity and tectonics of the Ninetyeast Ridge area: Evidence for internal deformation of the Indian plate. *Journal of Geophysical Research, 83*(B5), 2233-2245.
- Wiens, D. A., Stein, S., DeMets, C., Gordon, R. G., & Stein, C. (1986). Plate tectonic models for Indian Ocean. “intraplate” deformation. *Tectonophysics, 132*, 37-48.
- Wu, R.-S., & Aki, K. (1988). Multiple scattering and energy transfer of seismic waves-Separation of scattering effect from intrinsic attenuation II. Application of the theory to Hindu Kush region. *Pure and Applied Geophysics, 128*(1), 49-80.

APPENDIX

Selected earthquakes for the spectral analysis (sources; ANSS and ISC);

Magnitude (mb)	Date and Time (UTC)	Latitude	Longitude	Depth (km)	Epicentral Distance (km)
4	2010/07/25 - 09:35:03	6.6	76.78	10	440
4.1	2012/05/18 - 15:46:39	2.45	89.79	10	1142
4.2	2012/04/13 - 04:36:33	1.09	91.58	10	1390
4.2	2012/05/06 - 08:08:04	2.39	89.65	10	1131
4.2	2012/05/12 - 15:01:26	2.45	89.79	10	1142
4.3	2012/04/13 - 22:03:21	2.22	89.67	10	1143
4.3	2012/04/14 - 02:18:23	2.55	89.99	10	1156
4.3	2012/04/26 - 03:17:42	3.59	87.9	10	897
4.3	2012/05/19 - 22:29:31	2.35	89.8	10	1148
4.3	2012/04/13 - 22:58:56	1.89	89.69	10	1163
4.4*	2012/05/14 - 08:40:23	4.43	86.53	10	719
4.4	2012/04/14 - 04:03:49	2.47	90.43	10	1204
4.5	2012/05/09 - 07:30:39	4.84	87.9	10	842
4.5	2012/04/12 - 06.47.36	2.85	89.44	10	1087
4.5	2012/04/14 - 02.49.16	2.64	90.05	10	1158
4.5	2012/04/15 - 10.20.59	2.58	89.94	10	1150
4.5	2012/04/23 - 00.12.26	2.69	89.63	9	1114
4.5	2012/05/12 - 10.30.26	2.45	90.52	10	1214
4.5	2012/04/12 - 18.00.59	1.85	90.03	10	1198
4.6	2005/07/07 - 13:13:24	4.19	84.78	10	567
4.6	2007/01/28 - 00:18:52	7.76	88.37	10	848
4.6	2012/04/14 - 10:08:46	3.76	89.92	10	1094
4.6	2012/04/18 - 01:15:15	2.37	89.76	13	1143
4.6	2012/05/05 - 03:34:01	3.56	86.71	10	784
4.6	2012/05/07 - 21.31.35	2.33	89.79	10	1148
4.6	2012/05/13 - 12.30.59	2.54	90.51	17	1208
4.6	2012/04/13 - 19.52.06	1.57	91.24	10	1330
4.7	2011/11/19 - 10:40:16	3.92	79.02	10	417
4.7	2012/04/13 - 03:38:40	2.63	90.1	10	1163
4.7	2012/05/09 - 05:09:14	4.98	87.85	10	831
4.7	2012/04/13 - 14.29.06	2.22	90.26	10	1200
4.7	2012/04/13 - 04.49.49	1.55	91.04	10	1312
4.7	2012/04/18 - 17.50.27	2.62	90.32	15	1186
4.7	2012/04/29 - 02.13.56	2.22	89.79	13	1154
4.7	2012/05/09 - 14.27.15	2.29	89.76	7	1147
4.7	2012/05/15 - 00.25.40	1.53	89.98	10	1212
4.7	2012/06/14 - 10.58.26	2.7	91.41	13	1292
4.8	2001/01/27 - 19:22:45	3.49	74.9	20	769
4.8	2001/12/31 - 04:44:39	-2.57	83.3	10	1133
4.8	2002/02/26 - 01:50:42	3.41	86.38	10	762
4.8	2003/12/03 - 17:43:08	9.19	85.49	10	569
4.8	2012/04/19 - 06:30:11	1.42	90.86	10	1302
4.8	2012/05/30 - 17:21:18	3.35	88.29	10	948
4.8	2012/04/18 - 11.59.15	1.75	89.64	10	1167
4.8	2012/04/12 - 07.34.53	3.22	89.87	10	1112
4.8	2012/04/27 - 01.40.54	2.2	89.76	22	1152
4.9	2008/10/12 - 17:27:20	-3.33	81.68	10	1185
4.9	2008/10/16 - 04:28:45	-3.42	81.74	10	1196
4.9	2012/05/05 - 12:08:44	4.81	87.91	10	844
4.9	2012/04/13 - 12.48.12	3.4	89.94	10	1111
4.9	2012/04/15 - 13.57.42	1.88	90.9	10	1281
5	2007/01/17 - 07:58:41	1.98	89.69	10	1158
5	2012/04/13 - 05.31.46	2.65	89.71	14	1124
5.1	2012/05/04 - 16:23:43	2	89.72	10	1160
5.1	2012/04/14 - 12:18:26	2.59	90.35	10	1190
5.1	2012/05/15 - 05:19:56	2.71	89.56	10	1106
5.2	2007/07/18 - 04:27:24	6.47	84.39	10	417
5.3	2012/06/23 - 21:27:30	2.63	90.51	16	1204
5.4	2012/04/11 - 22:51:57	2.87	89.56	6	1097
5.4	2011/01/07 - 03:09:59	4.24	90.41	17	1127
5.5	2012/04/30 - 08:00:10	1.76	89.6	10	1162
5.5	2012/04/11 - 23:56:33	1.84	89.68	10	1165
5.5	2012/04/11 - 13:58:05	1.5	90.85	5	1296
5.7	2010/03/14 - 20:33:14	-2.75	83.7	15	1164
5.7	2012/04/11 - 11:53:36	2.91	89.54	10	1093

*event was available only in ISC